nature immunology

NK cells link obesity-induced adipose stress to inflammation and insulin resistance

Felix M Wensveen[1], Vedrana Jelenčić[1,6], Sonja Valentić[1,6], Marko Šestan[1,6], Tamara Turk Wensveen[2], Sebastian Theurich[3], Ariella Glasner[4], Davor Mendrila[5], Davor Štimac[2], F Thomas Wunderlich[3], Jens C Brüning[3], Ofer Mandelboim[4] & Bojan Polić[1]

An important cause of obesity-induced insulin resistance is chronic systemic inflammation originating in visceral adipose tissue (VAT). VAT inflammation is associated with the accumulation of proinflammatory macrophages in adipose tissue, but the immunological signals that trigger their accumulation remain unknown. We found that a phenotypically distinct population of tissue-resident natural killer (NK) cells represented a crucial link between obesity-induced adipose stress and VAT inflammation. Obesity drove the upregulation of ligands of the NK cell–activating receptor NCR1 on adipocytes; this stimulated NK cell proliferation and interferon-γ (IFN-γ) production, which in turn triggered the differentiation of proinflammatory macrophages and promoted insulin resistance. Deficiency of NK cells, NCR1 or IFN-γ prevented the accumulation of proinflammatory macrophages in VAT and greatly ameliorated insulin sensitivity. Thus NK cells are key regulators of macrophage polarization and insulin resistance in response to obesity-induced adipocyte stress.

With an estimated half a billion obese and 1 billion overweight people worldwide[1], overt metabolic dysregulation is one of the most pressing health challenges of our time. An important complication in obesity is insulin resistance, which can ultimately lead to diabetes mellitus type 2, a major global cause of morbidity and mortality[2]. A primary underlying cause of obesity-induced insulin resistance is chronic systemic inflammation originating in the visceral adipose tissue (VAT)[3–5]. In lean individuals, various immune cell subsets, including eosinophils, type 2 innate lymphoid cells (ILC2 cells) and invariant natural killer T cells (*i*NKT cells)[6–9], are important in maintaining VAT homeostasis. These cells secrete type 2 helper T cell (T_H2)-type cytokines, such as interleukin 5 (IL-5) and IL-13, and thereby prevent the formation, accumulation and activation of proinflammatory immune cells, most importantly of macrophages.

Obesity deregulates homeostasis in VAT by inducing changes in the endocrinological signals and the composition of metabolites that reach it from the peripheral adipose tissue[10,11]. In addition, obesity-induced hypertrophy of adipocytes limits their access to oxygen and nutrients[12,13]. The resulting stress responses of adipocytes and stromal cells lead to the activation and accumulation of proinflammatory cells in VAT[5]. Obesity-induced inflammation of VAT drives an influx of T_H1 $CD4^+$ T cells, $CD8^+$ T cells and B cells, generating a T_H1-type immune response that is aggravated over time as more factors and cells become involved[14–16]. This results in chronic systemic production of proinflammatory cytokines, such as tumor necrosis factor (TNF) and IL-1β, which in time reduces systemic insulin sensitivity[17]. However, how adipose tissue stress is translated into a signal that activates the immune system is largely unknown.

An important early event in VAT inflammation is the activation of macrophages in adipose tissue. Under lean conditions, adipose tissue–resident macrophages have an anti-inflammatory (M2)-like phenotype. After high-fat feeding, macrophages rapidly increase in number and develop proinflammatory (M1)-like features[3,4]. Although many cells in the VAT of obese subjects are able to produce proinflammatory mediators[15,16], adipose tissue macrophages are considered to be the dominant source of IL-1β and TNF and to be pivotal for the development of obesity-induced insulin resistance[18]. Whereas much is known about the factors that stimulate the increase in the number of macrophages, it is still unclear how the M2-to-M1 transition is initiated, especially in the absence of overt microbial infection.

Natural killer (NK) cells are important sentinels of the body that survey tissues for infected, transformed or otherwise 'stressed' cells. They are armed with a number of activating and inhibitory receptors that are calibrated to detect different signs of cytopathology while ensuring self-tolerance[19]. Downregulation of major histocompatibility complex class I molecules (the so-called 'missing self') or upregulation of stress ligands for activating NK cell receptors ('induced self') on target cells stimulates NK cells to produce cytokines such as interferon-γ (IFN-γ) or mediate a cytolytic response[20]. NKp46 (NCR1 in mice) is a particularly potent activating receptor on NK cells that is important in the defense against influenza infection[21], as well as in

[1]Department of Histology and Embryology, Faculty of Medicine, University of Rijeka, Rijeka, Croatia. [2]Department of Internal Medicine, University Hospital Rijeka, Rijeka, Croatia. [3]Max Planck Institute for Metabolism Research Cologne, Cologne, Germany. [4]The Lautenberg Center for General and Tumor Immunology, The Hebrew University Hadassah Medical School, Jerusalem, Israel. [5]Department of Surgery, University Hospital Rijeka, Rijeka, Croatia. [6]These authors contributed equally to this work. Correspondence should be addressed to B.P. (bojan.polic@medri.uniri.hr).

Received 16 December 2014; accepted 9 February 2015; published online 2 March 2015; doi:10.1038/ni.3120

the development of diabetes mellitus type 1 (ref. 22). The role of NK cells in the development of type 2 diabetes is still unclear.

Cytokines produced by immune cells are required for macrophages to switch from a homeostatic to an inflammatory state[23]. In infected tissues, NK cell–derived IFN-γ was shown to be indispensable for M1 macrophage polarization[24]. Importantly, *in vitro* IFN-γ–stimulated macrophages develop a phenotype similar to that of M1 adipose tissue–resident macrophages[25]. Accordingly, IFN-γ ablation reduces the development of obesity-associated insulin resistance[26–28].

Here we demonstrate that VAT-resident NK cells are crucial to the connections among obesity-induced adipose stress, macrophage activation and insulin resistance. Obesity-induced adipose stress caused upregulation of NCR1 ligands on adipocytes, which activated VAT-resident NK cells and promoted their proliferation. IFN-γ produced by these cells in response to NCR1 signaling induced M1 macrophage differentiation. When NK cell activation was prevented, obesity-induced M1 macrophage polarization was strongly reduced, resulting in ameliorated glucose tolerance and insulin sensitivity. Our study delineates one of the primary mechanisms by which obesity-induced adipose stress is translated into an immunological signal that drives M1 macrophage formation and leads to insulin resistance.

RESULTS

High-fat diet increases NK cell IFN-γ production in VAT

IFN-γ deficiency protects mice from diet-induced insulin resistance, but its exact role in this process is unclear[26–28]. To determine whether IFN-γ has an early role in the induction of insulin resistance, we measured IFN-γ expression in the VAT of mice with diet-induced obesity (DIO). IFN-γ expression was considerably higher in the VAT of mice fed a high-fat diet (HFD) for 4 weeks than in mice receiving a normal chow diet (NCD; **Fig. 1a**). *In vitro* stimulation of leukocytes in VAT showed that in the lean tissue, NK cells and T cells together represented >95% of all IFN-γ–producing cells in VAT, whereas macrophages and B cells did not produce IFN-γ (**Supplementary Fig. 1a**,**b**). Among the leukocytes isolated from mouse VAT after 4 weeks of high-fat feeding, NK cells represented ~47% of the IFN-γ–producing population, compared with ~39% in fat from lean mice (**Fig. 1b**).

Tissue-specific NK cell subsets have been characterized[20]. Our quantification of VAT leukocytes showed that NK cells represented ~13% of immune cells (CD45$^+$) in the lean adipose tissue (**Fig. 1c**). Similar to splenic NK cells, VAT NK cells expressed the early developmental markers NK1.1, NKG2D and NCR1 (**Fig. 1d** and **Supplementary Fig. 1c**) and, after *in vitro* stimulation, had cytotoxic and proliferative capacities similar to those of splenic NK cells (**Supplementary Fig. 1d–f**). Compared with splenic NK cells, VAT NK cells had lower expression of terminal differentiation markers (for example, CD11b and KLRG1)[29]; had lower expression of the Ly49 molecules h, g2, d and i; expressed greater amounts of CD27; and had lower expression of the adhesion molecules CD62L and DX5 (**Supplementary Fig. 1c**). NK cells and ILC1 cells are developmentally closely related. VAT NK cells expressed several markers that are also expressed by ILC1 cells in the small intestine, such as CD49a and CD69, whereas they had low expression of the transcription factor Eomes[30]. However, they did not express CD127 and the stem cell factor receptor c-Kit, which define ILC1 cells[30]. Moreover, VAT NK cells had lower expression of CD122 and T-bet than did NK cells in spleen (**Fig. 1d**), which suggests that VAT NK cells are a phenotypically distinct, tissue-specific population.

We next compared the VAT-resident NK cell response to high-fat feeding with that of other immune cell subsets that have been implicated in obesity-induced insulin resistance. Within 2 weeks after the start of high-fat feeding, numbers of both macrophages and NK cells increased threefold to fivefold in the VAT, but not in the spleen, whereas numbers of *i*NKT cells and γδ T cells remained unchanged for the first 4 weeks relative to the amounts measured at the beginning of the HFD (**Fig. 1e** and **Supplementary Fig. 1g**,**h**). In contrast, the reported increase in the number of CD8$^+$ T cells and reduction in the number of regulatory T cells[16,31] in response to the HFD appeared

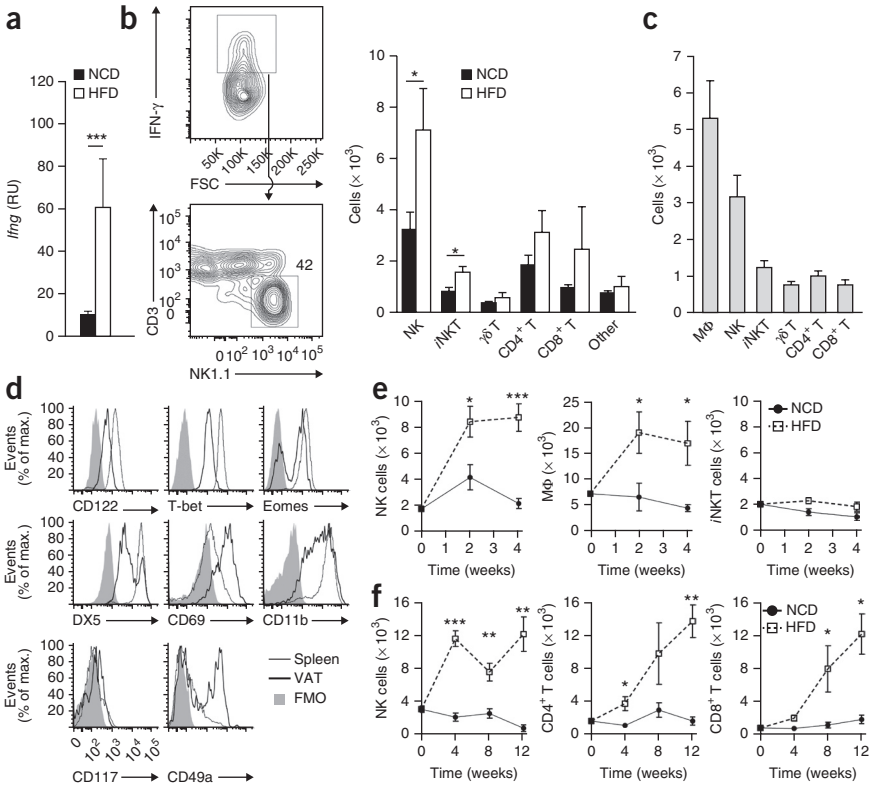

Figure 1 A high-fat diet increases IFN-γ production by NK cells in VAT. (**a**) Results of quantitative PCR analysis showing transcript expression of *Ifng* in VAT tissue homogenates of mice fed an NCD or an HFD for 4 weeks ($n = 9$). RU, relative units. (**b**) Flow cytometry of IFN-γ–expressing cells in VAT after *in vitro* stimulation with the phorbol ester PMA and ionomycin after 4 weeks of NCD or HFD feeding ($n = 4$–5). FSC, forward scatter. The number "42" adjacent to the outlined area in the lower panel represents the percentage of cells in the gate. (**c**) Number of cells per epididymal fat pad in lean mice ($n = 10$). MΦ, macrophage. (**d**) Flow cytometry of protein expression in VAT-resident NK cells. Gated for CD3$^-$NK1.1$^+$ cells. FMO, fluorescence minus one. (**e**,**f**) Kinetics of immune cells in the VAT of mice fed with an NCD or an HFD ($n = 5$). $^*P < 0.05$, $^{**}P < 0.01$, $^{***}P < 0.001$ (Mann-Whitney and Student's *t*-test). Data (±s.e.m.) are representative of two (**e**,**f**), five (**b**) or seven (**c**,**d**) independent experiments. Panel **a** shows pooled data from three experiments.

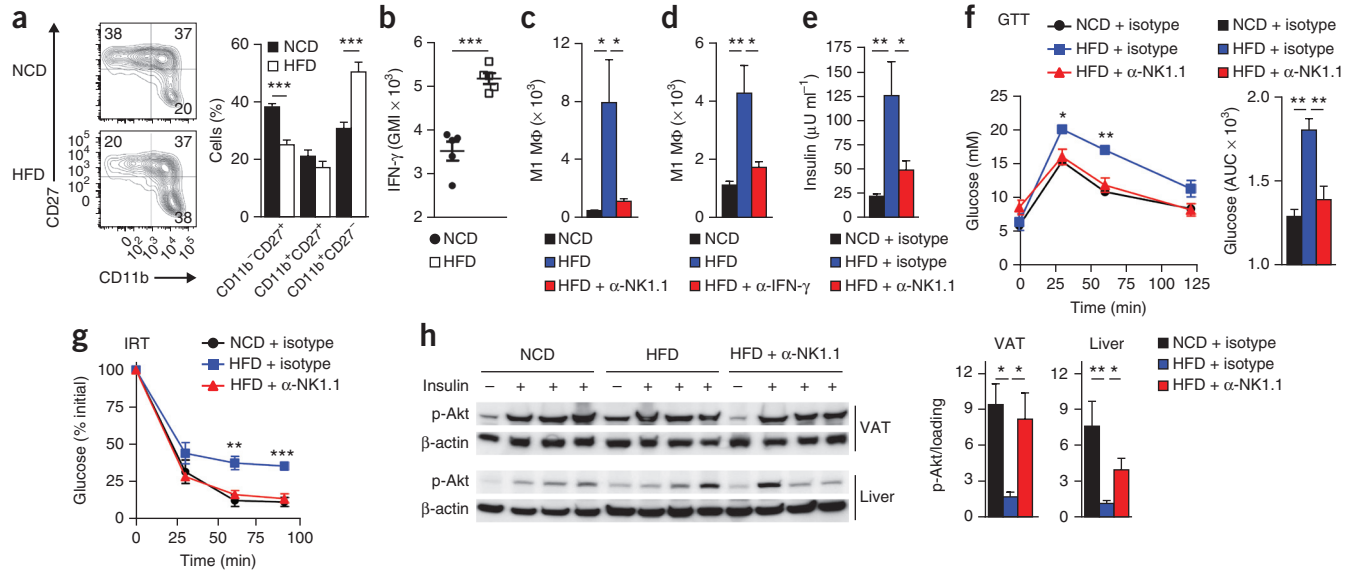

Figure 2 VAT-resident NK cells are activated by HFD feeding and promote insulin resistance. (**a**) Flow cytometric analysis of NK cells after NCD or HFD feeding for 4 weeks. Cells were gated for $CD3^-NK1.1^+NCR1^+$ cells ($n = 5$). Numbers in quadrants (right) indicate the percentage of cells in each. (**b**) Results of intracellular flow cytometric analysis of IFN-γ production by VAT NK cells upon *in vitro* stimulation with PMA and ionomycin after 4 weeks of NCD or HFD feeding ($n = 5$). GMI, geometric mean intensity of fluorescence. (**c**) Total number of M1 macrophages ($CD19^-CD11b^+F4/80^+GR1^{Dim/-}CD11c^+CD86^{Dim}$) in VAT of NCD- or HFD-fed mice (6 weeks). Mice received PBS or depleting α-NK1.1 antibodies every 5 d ($n = 4$–5). (**d**) Total number of M1 macrophages in VAT of NCD- or HFD-fed mice (6 weeks). Mice received PBS or neutralizing IFN-γ antibodies via i.p. injection once every other day ($n = 5$). (**e**–**h**) Mice were NCD- or HFD-fed (12 weeks) and received depleting α-NK1.1 or isotype control antibodies every 5 d ($n = 5$–7). (**e**) Results of serum ELISA showing insulin concentrations. (**f**) Glucose tolerance test (GTT) was accomplished by i.p. injection of glucose (1 g kg^{-1}) and measurement of blood glucose concentration by glucometer after overnight fasting. Shown are plasma glucose concentrations and area under the curve (AUC). (**g**) Insulin resistance test (IRT) was done by i.p. injection of insulin (1.0 U kg^{-1}) and measurement of blood glucose concentrations. (**h**) Mice were fasted overnight and injected intraperitoneally with either PBS (–) or 1.0 U kg^{-1} insulin (+). Immunoblotting was used to quantify phosphorylated Akt (phosphorylated at Ser473; p-Akt) in tissue samples of liver and VAT. β-actin was used as a loading control. Quantification shows pooled data from two independent experiments. Protein expression relative to unstimulated cells is given. $^*P < 0.05$, $^{**}P < 0.01$, $^{***}P < 0.001$ (Student's *t*-test and analysis of variance (ANOVA) with Bonferroni's post-test). Data (±s.e.m.) are representative of four (**b**–**g**) or five (**a**) independent experiments. Panel **h** shows pooled data from three experiments.

after 8 weeks of feeding (**Fig. 1f** and **Supplementary Fig. 1i**), which suggests that T cells are probably not the main source of IFN-γ during the early induction of IFN-γ in obese VAT. Thus, the production of IFN-γ was increased in VAT early (at 4 weeks) during feeding with an HFD and was primarily associated with the expansion of an $IFN\text{-}\gamma^+$ VAT-resident NK cell population.

HFD activates NK cells and drives M1 macrophage polarization

Next we investigated whether NK cells are involved in M1-like macrophage polarization in the early stages of high-fat feeding. After 4 weeks, VAT NK cells in mice fed an HFD acquired a more activated ($CD11b^+$) phenotype and produced more IFN-γ than NK cells in NCD-fed animals (**Fig. 2a**,**b**). After 4 weeks of feeding, we did not note a higher percentage of $CD4^+$ helper T cells that produced IFN-γ in HFD-fed mice compared with NCD-fed mice, and T_H17 cells were hardly detectable in the VAT of either NCD- or HFD-fed mice (**Supplementary Fig. 2a**). We next investigated the effect of NK cell depletion on the accumulation of M1-like macrophages during feeding with an HFD by using NK1.1 antibodies. Because the NK1.1 receptor is expressed on other cell types, we used a low-dose NK1.1-antibody depletion protocol[32] that reduced NK cell numbers by more than tenfold but did not have a considerable effect on the numbers of $NK1.1^+$ NKT cells and $CD8^+$ T cells (**Supplementary Fig. 2b**). Similar to classical M1 macrophages, VAT-resident M1 macrophages had high expression of integrin CD11c and inducible nitric oxide synthase (iNOS) and low expression of the costimulatory molecule CD86, arginase and IL-4Rα (**Supplementary Fig. 2c**,**d**). Compared with NCD feeding, 6 weeks of feeding with an HFD resulted in 19-fold more M1 macrophages in VAT; in contrast, the number of M1 macrophages in HFD-fed mice in which NK cells had been depleted was not increased (**Fig. 2c**).

Total macrophage numbers were lower in NK cell–depleted mice than in untreated mice on an HFD, and M1 macrophage numbers decreased to the greatest extent. The relative increase in numbers of M1 over M2 macrophages in HFD-fed mice compared with mice on a normal diet was not seen in α-NK1.1–treated HFD-fed mice (**Supplementary Fig. 2e**). This indicates that NK cells primarily affect the polarization and, to a lesser extent, the proliferation of VAT macrophages. In addition, antibody-mediated neutralization of IFN-γ prevented the HFD-induced accumulation of M1 macrophages and an increase in the ratio of M1 macrophages to M2 macrophages (**Fig. 2d** and **Supplementary Fig. 2f**). IFN-γ neutralization did not prevent an increase in the number of $CD11b^+$ NK cells in VAT in response to HFD feeding (**Supplementary Fig. 2g**), which indicates that IFN-γ production is downstream of NK cell activation.

Next, we investigated whether NK cell depletion prevented the clinical complications of diet-induced obesity. NK cell–depleted mice did not show hyperinsulinemia after 12 weeks of an HFD, in contrast to non-NK cell–depleted mice (**Fig. 2e**). In NK cell–deficient mice, glucose tolerance and systemic insulin sensitivity were ameliorated enough to be comparable to those in NCD-fed mice (**Fig. 2f**,**g**). Liver and VAT cells from HFD-fed mice showed reduced induction of phospho-serine-threonine kinase (p-Akt) and phospho-p70 (p-p70) in response to insulin compared with amounts in

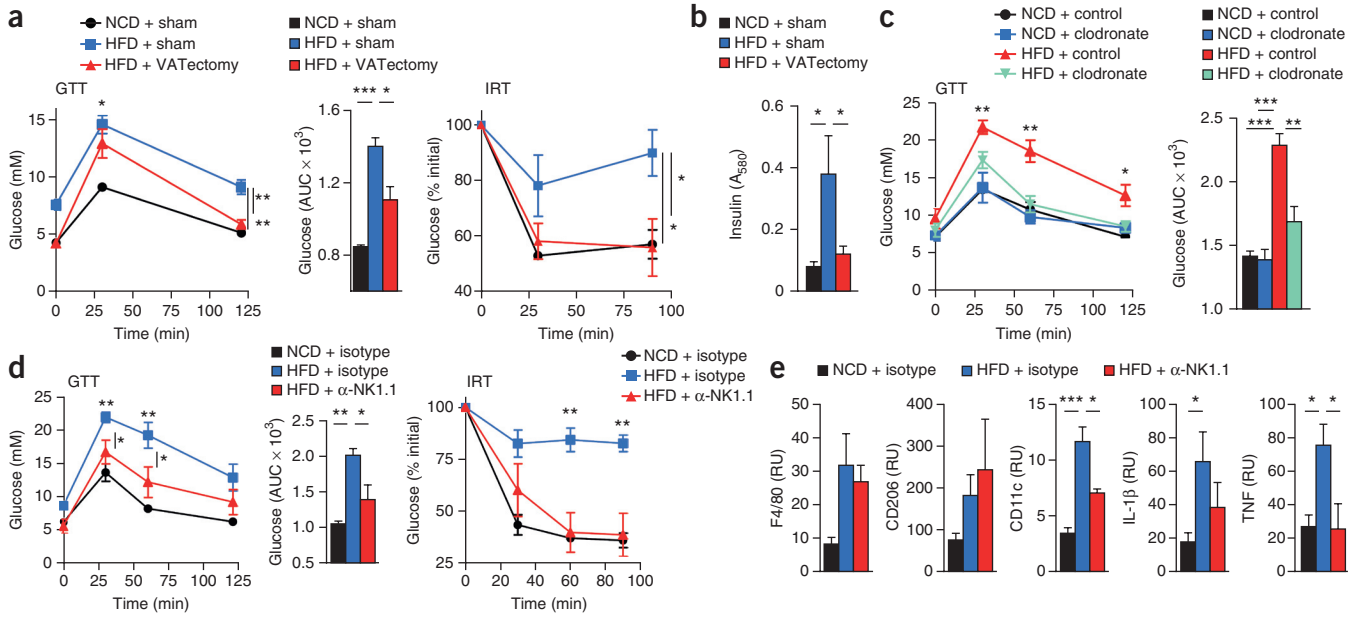

Figure 3 VAT NK cells are required and sufficient for the induction of insulin resistance. (**a**,**b**) Mice either underwent sham operation or had abdominal fat removed (VATectomy). Two weeks after surgery, mice began NCD or HFD feeding, and 12 weeks later they were subjected to (**a**) GTT and IRT (shown are plasma glucose concentrations and AUC) and (**b**) measurement of serum insulin levels as determined by ELISA ($n = 3–5$). (**c**) Mice were NCD- or HFD-fed and received clodronate-loaded or control liposomes every 2 weeks. After 10 weeks, mice were subjected to GTT. Shown are plasma glucose concentrations and AUC ($n = 3–5$). (**d**) *Prkdc*^{scid} (SCID) mice were NCD- or HFD-fed for 12 weeks and received depleting α-NK1.1 or isotype control antibodies every 5 d. After 12 weeks, mice were subjected to GTT and IRT. Shown are plasma glucose concentrations and AUC ($n = 3–5$). (**e**) SCID mice were NCD- or HFD-fed for 12 weeks and received PBS or depleting α-NK1.1 antibodies every 5 d. Total RNA was isolated from VAT, and relative gene expression was determined by quantitative PCR ($n = 3–5$). RU, relative units. $^*P < 0.05$, $^{**}P < 0.01$, $^{***}P < 0.001$ (ANOVA with Bonferroni's post-test). Data (±s.e.m.) are representative of one (**c**) or two (**a**,**b**,**d**,**e**) independent experiments.

NCD-fed animals, whereas depletion of NK cells normalized these values (**Fig. 2h** and **Supplementary Fig. 2h**,**i**). Obesity-induced weight gain, in contrast, was not affected by NK cell depletion (**Supplementary Fig. 2j**,**k**), which indicated that NK cells affect inflammation rather than VAT metabolism directly. All together, these data show that NK cells are important in the accumulation of M1 macrophages in VAT and the development of obesity-induced insulin resistance.

VAT NK cells are required for HFD-induced insulin resistance

To show that VAT, rather than other organs or tissues, is required for the development of insulin resistance in obese mice, we subjected the mice to surgical excision of visceral adipose fat pads (VATectomy) 2 weeks before the initiation of HFD feeding. Twelve weeks after VATectomy, we found normal glucose-tolerance responses in NCD-fed mice compared with mice that had undergone sham operation. HFD feeding resulted in a large increase in the mass of subcutaneous adipose tissue in VATectomized mice compared with HFD-fed animals that underwent sham operation (**Supplementary Fig. 3a**,**b**). HFD-fed VATectomized mice did not develop insulin resistance or hyperinsulinemia in this time frame (**Fig. 3a**,**b**); these mice did develop greater glucose intolerance than NCD-fed controls, but it was significantly less than that in HFD-fed mice that underwent sham operation (**Fig. 3a**). Taken together, these data indicate that VAT is the primary tissue responsible for the generation of obesity-induced insulin resistance and glucose intolerance.

Next, we investigated whether macrophages in adipose tissue promoted the induction of glucose intolerance in response to an HFD. Consistent with published reports[33], we observed significantly improved glucose tolerance in mice in which macrophage function was disturbed by the administration of clodronate-loaded liposomes compared with mice to which control liposomes had been administered (**Fig. 3c**). Thus, macrophages in adipose tissue were important for HFD-induced glucose intolerance in our model.

To investigate whether VAT NK cells are sufficient to promote the accumulation of M1 macrophages in adipose tissue in the absence of T cells, we fed an HFD to mice with severe combined immunodeficiency (SCID). SCID mice are deficient for the DNA-PK protein kinase subunit DNA-PKcs, which is essential for V(D)J recombination, and they therefore lack T and B cells[34]. As a note, SCID mice also have defects in hepatic lipogenesis[35], which might represent a limitation for their use in this particular context, but they do gain weight in response to an HFD and develop insulin resistance[36]. After 14 weeks on an HFD, SCID mice showed impaired glucose tolerance and developed insulin resistance similar to that seen in wild-type mice on the same diet, indicating that the innate immune system is sufficient for the development of this condition (**Supplementary Fig. 3c**). Moreover, NK cell activation, as measured by the induction of CD11b and KLRG1 on these cells, was still observed in the VAT of HFD-fed SCID mice (**Supplementary Fig. 3d**), which suggests that adaptive immune cells are not required for this step. NK cell depletion also significantly improved glucose tolerance and insulin sensitivity in HFD-fed SCID mice, which corresponded with a reduction in the number of M1 macrophage cells compared with that in HFD-fed SCID mice in which NK cells were not depleted (**Fig. 3d** and **Supplementary Fig. 3e**). Depletion of NK cells did not alter the amount of obesity-induced weight gain in HFD-fed SCID mice (**Supplementary Fig. 3f**,**g**). Quantitative PCR analysis of VAT tissue homogenates from these

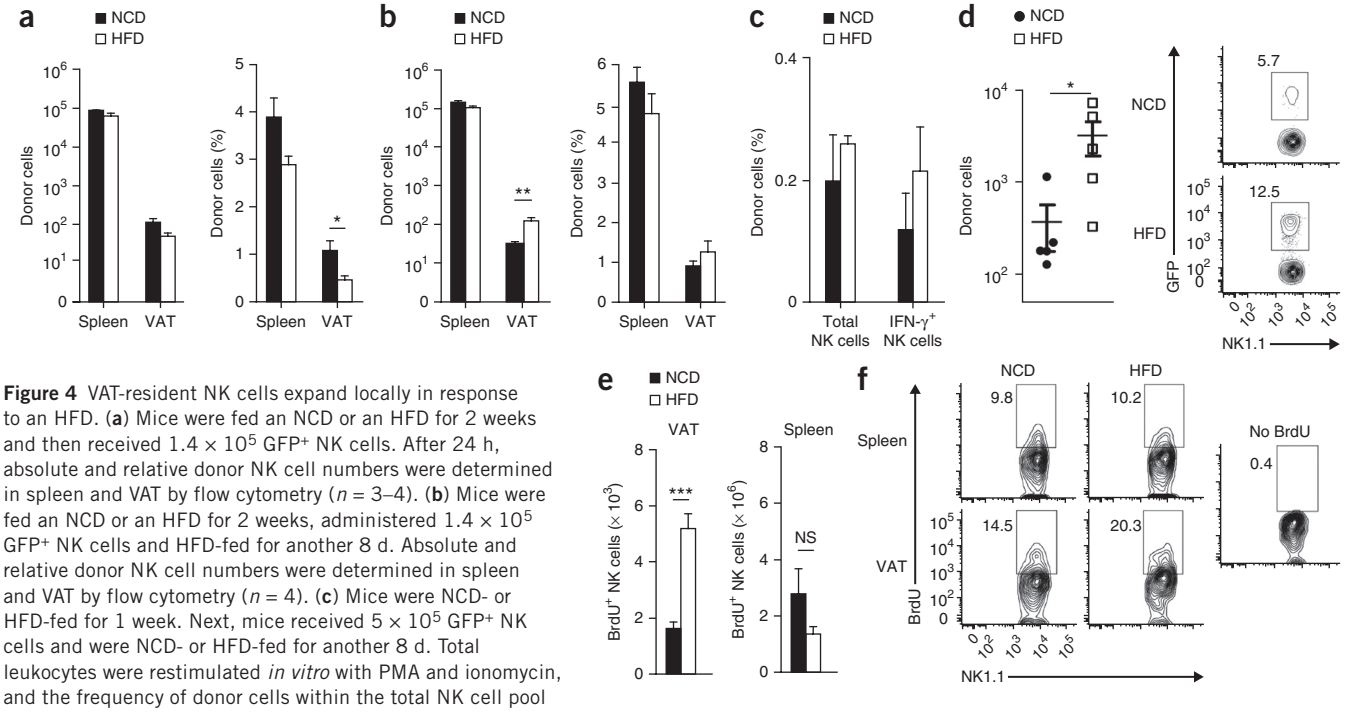

Figure 4 VAT-resident NK cells expand locally in response to an HFD. (**a**) Mice were fed an NCD or an HFD for 2 weeks and then received 1.4×10^5 GFP$^+$ NK cells. After 24 h, absolute and relative donor NK cell numbers were determined in spleen and VAT by flow cytometry ($n = 3$–4). (**b**) Mice were fed an NCD or an HFD for 2 weeks, administered 1.4×10^5 GFP$^+$ NK cells and HFD-fed for another 8 d. Absolute and relative donor NK cell numbers were determined in spleen and VAT by flow cytometry ($n = 4$). (**c**) Mice were NCD- or HFD-fed for 1 week. Next, mice received 5×10^5 GFP$^+$ NK cells and were NCD- or HFD-fed for another 8 d. Total leukocytes were restimulated *in vitro* with PMA and ionomycin, and the frequency of donor cells within the total NK cell pool and in the IFN-γ$^+$ NK cell pool was determined by flow cytometry ($n = 3$). (**d**) Wild-type mice were fed an NCD or an HFD. After 5 weeks, 3×10^5 GFP$^+$ NK cells were injected into the fat pads of the mice. The total number of donor NK cells (CD3$^-$NK1.1$^+$GFP$^+$) in VAT was quantified by flow cytometry. Representative plots were gated for CD3$^-$NK1.1$^+$NCR1$^+$ cells ($n = 5$). (**e**,**f**) Mice were NCD- or HFD-fed for 2 weeks and received BrdU every other day during the last 8 d of feeding ($n = 4$). (**e**) BrdU$^+$ NK cells were quantified in spleen and VAT by flow cytometry. NS, not significant. (**f**) Representative plots were gated for CD3$^-$NK1.1$^+$NCR1$^+$ cells. Numbers adjacent to outlined areas in **d** and **f** represent the percentages of cells in gates. $^*P < 0.05$, $^{**}P < 0.01$, $^{***}P < 0.001$ (Student's *t*-test). Data (± s.e.m.) are representative of one (**c**), two (**e**) or three (**a**,**b**,**d**) independent experiments.

mice showed that expression of the macrophage marker F4/80 and the M2 polarization marker CD206 was induced in VAT in response to the HFD (**Fig. 3e**), even though differences did not reach statistical significance. The increased number of F4/80$^+$ cells in HFD-fed SCID mice compared with that in NCD-fed mice was confirmed by flow cytometry (**Supplementary Fig. 3e**). In contrast, expression of the M1 polarization marker CD11c was notably increased in HFD-fed SCID mice only when NK cells were present. Consistent with the effects of NK cells on M1 macrophage accumulation, the expression of proinflammatory cytokines such as IL-1β and TNF was significantly increased in HFD-fed mice compared with that in NCD-fed controls, but only in the presence of NK cells. Thus, NK cells are both required and sufficient to promote obesity-induced M1 macrophage accumulation, inflammation and insulin resistance.

HFD drives the local proliferation of NK cells in VAT

Many tissues in humans and mice contain specialized resident NK cell subsets that aid in local immune responses independent of peripheral immunity[20]. Because NK cells were present in particularly high amounts in VAT (~13% of leukocytes) relative to the amounts in most other tissues (spleen, ~3%: liver, ~8%; brown adipose tissue, ~4%; and subcutaneous fat, ~13%) under lean conditions (**Supplementary Fig. 4a**,**b**), we investigated whether the HFD-induced increase in the number of NK cells in VAT was due to an influx of peripheral cells or local expansion. After being fed with an NCD or an HFD for 2 weeks, mice received i.v. injections of splenic GFP$^+$ NK cells from wild-type NCD-fed mice, and the frequency of donor (GFP$^+$) cells was quantified 1 d after transfer. A considerable fraction (~6%) of NK cells in spleen were donor cell derived; however, very few GFP$^+$ cells (~1% of total NK cells) could be detected in the VAT of NCD- or HFD-fed mice (**Fig. 4a**). The number of donor GFP$^+$ NK cells in the VAT was similar in HFD-fed and NCD-fed recipient mice. Because the VAT of mice fed an HFD contained more NK cells than lean tissue, this resulted in relatively fewer donor NK cells in obese VAT (**Fig. 4a**). Next, splenic NK cells were transferred intravenously into mice fed an NCD or an HFD for 2 weeks before cell transfer, and the number of donor NK cells was quantified in VAT 8 d after transfer. HFD-fed recipient mice had threefold to fourfold more donor GFP$^+$ NK cells than did NCD-fed recipients (**Fig. 4b**). Whereas 1 d after transfer donor cells constituted only ~0.5% of the total number of NK cells, after 8 d this had increased to ~1.2% (**Fig. 4a**,**b**). This indicates that peripheral influx in the VAT is not promoted as a result of HFD feeding, but cells that do reach the VAT proliferate faster than tissue-resident cells. *In vitro* stimulation showed that donor NK cells did not contribute more to the IFN-γ$^+$ NK cell population than to the total NK cell population in the VAT of either NCD-fed or HFD-fed mice (**Fig. 4c**), which indicated that infiltrating peripheral NK cells were functionally equivalent to resident NK cells under HFD conditions. Next, GFP$^+$ NK cells were injected directly into the fat pads of lean and obese animals. Donor GFP$^+$ NK cells engrafted into the VAT in both HFD-fed and NCD-fed recipients, but HFD-fed recipients had significantly more donor GFP$^+$ NK cells in VAT than did NCD-fed recipients ($P < 0.05$; **Fig. 4d**). These data confirmed that fat in obese subjects generated a local environment that supported greater numbers of NK cells.

To determine whether the increase in the number of NK cells in VAT in response to the HFD was due to local NK cell proliferation, we fed mice with an NCD or an HFD for 2 weeks and administered i.p. injections of 5-bromodeoxyuridine (BrdU) every second day for the last 8 d of the feeding period. Similar numbers of BrdU$^+$ NK cells

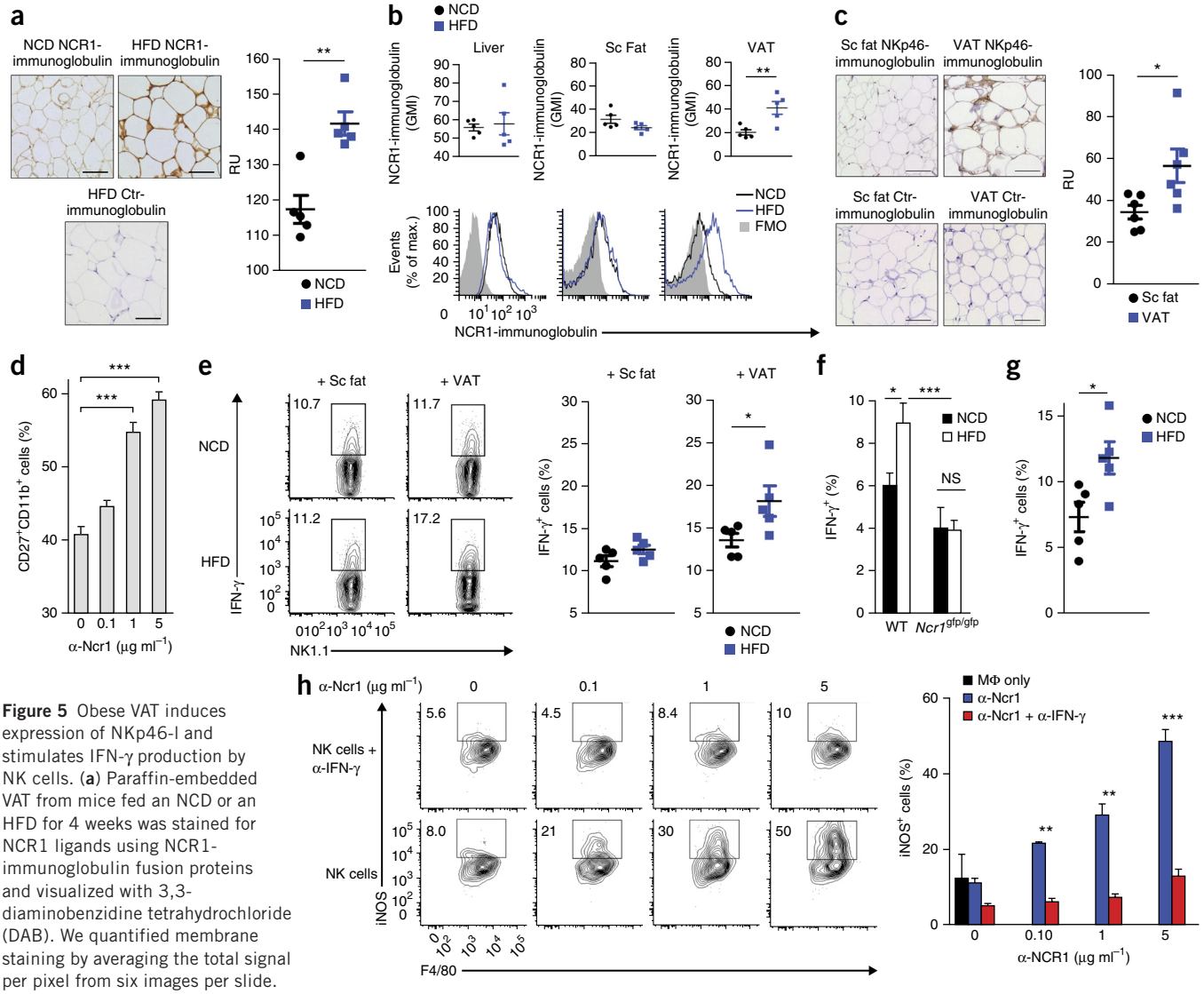

Figure 5 Obese VAT induces expression of NKp46-I and stimulates IFN-γ production by NK cells. (**a**) Paraffin-embedded VAT from mice fed an NCD or an HFD for 4 weeks was stained for NCR1 ligands using NCR1-immunoglobulin fusion proteins and visualized with 3,3-diaminobenzidine tetrahydrochloride (DAB). We quantified membrane staining by averaging the total signal per pixel from six images per slide. Scale bars, 100 μm. Irrelevant fusion proteins were used as negative controls ($n = 5$). (**b**) Total hepatocytes and purified mature adipocytes isolated from subcutaneous (Sc) fat and VAT were stained with NCR1-immunoglobulin fusion proteins and analyzed by low-pressure flow cytometry. Gated for $CD45^-$ cells ($n = 5$). (**c**) Human VAT and Sc fat sections were stained with hNKp46-immunoglobulin fusion proteins and visualized with DAB ($n = 6$). Irrelevant fusion proteins were used as negative controls (scale bars, 100 μm). RU, relative units. (**d**) Fraction of $CD27^+CD11b^+$ cells within NK cells stimulated for 2 d with agonistic NCR1 antibodies and analyzed by flow cytometry ($n = 3$). (**e**) NK cells were stimulated with the cell-membrane fraction of purified mature adipocytes isolated from Sc fat and VAT. IFN-γ production was analyzed by flow cytometry. Gated for $CD3^-NK1.1^+NCR1^+$ cells ($n = 5$). (**f**) Wild-type (WT) and NCR1-deficient ($Ncr1^{gfp/gfp}$) NK cells were stimulated with the cell-membrane fraction of purified mature adipocytes isolated from NCD- or HFD-fed mice. IFN-γ production was analyzed by flow cytometry ($n = 6$). (**g**) IFN-γ production by VAT NK cells measured by flow cytometry upon *in vitro* NCR1 stimulation by agonistic antibodies after 3 weeks of NCD or HFD feeding ($n = 5$). (**h**) Macrophages were left unstimulated ("MΦ only") or cocultivated with NK cells activated with agonistic NCR1 antibodies in the presence or absence of neutralizing IFN-γ antibodies. After 2 d, intracellular iNOS production of macrophages was assessed by flow cytometry. Gated for $CD19^-CD11b^+F4/80^+GR1^{-/Dim}$ cells ($n = 3$). Numbers adjacent to outlined areas in **e** and **h** represent the percentages of cells in gates. $^*P < 0.05$, $^{**}P < 0.01$, $^{***}P < 0.001$ (Student's *t*-test). Data (±s.e.m.) are representative of one (**c**), two (**a**,**b**), three (**h**), four (**d**,**e**) or five (**g**) independent experiments. Panel **f** shows pooled data from two experiments.

($CD3^-NK1.1^+NCR1^+$) were found in the spleens of HFD-fed mice and NCD-fed controls (**Fig. 4e**). In contrast, threefold to fourfold more $BrdU^+$ NK cells were detected in the VAT of HFD-fed mice than in that of NCD-fed mice (**Fig. 4e**,**f**). To exclude an effect of differential NK cell survival and/or efflux from tissues, we also assessed BrdU incorporation in VAT NK cells of NCD-fed or HFD-fed mice 4 h after BrdU injection. At this time point as well, more $BrdU^+$ NK cells ($CD3^-NK1.1^+NCR1^+$) were detected in obese VAT than in lean VAT (**Supplementary Fig. 4c**). These observations suggest that, as with adipose tissue macrophages[37], the obesity-induced increase in the number of NK cells in the VAT is probably primarily due to local proliferation.

Stressed adipocytes activate NK cells via NCR1 ligands

Stressed tissues induce the expression of cell-surface proteins that attract and activate NK cells[38]. Induced expression of ligands for the NK cell–activating receptor NCR1 on pancreatic beta cells promotes type 1 diabetes in mice[22]. Unfortunately, the exact identities of NCR1 ligands are currently unknown, but they can be detected using NCR1-immunoglobulin fusion proteins[22]. We therefore investigated whether

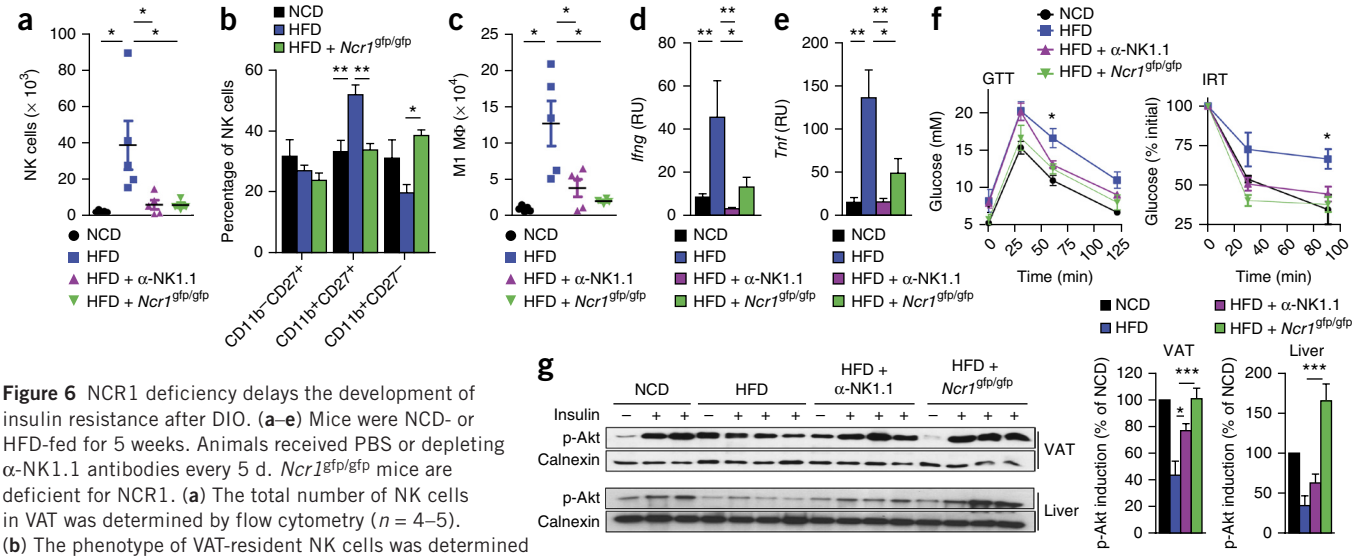

Figure 6 NCR1 deficiency delays the development of insulin resistance after DIO. (**a**–**e**) Mice were NCD- or HFD-fed for 5 weeks. Animals received PBS or depleting α-NK1.1 antibodies every 5 d. *Ncr1*$^{gfp/gfp}$ mice are deficient for NCR1. (**a**) The total number of NK cells in VAT was determined by flow cytometry ($n = 4–5$). (**b**) The phenotype of VAT-resident NK cells was determined by flow cytometry ($n = 4–5$). Cells of NK-depleted mice were not analyzed. (**c**) The total number of M1 macrophages was determined by flow cytometry ($n = 4–5$). (**d**) Expression of *Ifng* ($n = 4–13$) and (**e**) *Tnf* in the VAT of mice was determined by quantitative PCR of whole tissue homogenates ($n = 4–5$). (**f**,**g**) The indicated groups of mice were NCD- or HFD-fed for 12 weeks and (**f**) subjected to GTT and IRT ($n = 4–5$). (**g**) Mice were fasted overnight and injected intraperitoneally with either PBS (–) or 1.0 U kg^{-1} insulin (+). Immunoblotting was used to quantify phosphorylated Akt (phosphorylated at Ser473; p-Akt) in tissue samples of liver and VAT. Calnexin was used as a loading control. p-Akt induction in PBS-injected controls relative to NCD-fed animals is given ($n = 2–3$). Data (±s.e.m.) are representative of two (**e**,**g**) or three (**a**–**c**,**f**) independent experiments. Panel **d** shows pooled data from three experiments. $^*P < 0.05$, $^{**}P < 0.01$, $^{***}P < 0.001$ (ANOVA with Bonferroni's post-test).

the expression of NCR1 ligands is induced in obese VAT by means of immunohistological analysis. Similar to what was observed in pancreatic beta cells in Langerhans islets[22], low expression of NCR1 ligands was detected on adipocytes in lean mouse VAT, whereas adjacent tissues, such as in the epididymis, were negative for these molecules (**Fig. 5a** and **Supplementary Fig. 5a**). In the immunohistological analysis, adipocytes in VAT of HFD-fed mice showed increased expression of ligands for NCR1 but not of ligands for NKG2D, another activating stress receptor on NK cells (**Fig. 5a** and **Supplementary Fig. 5a**). Flow cytometric analysis showed that adipocytes from VAT induced NCR1-l expression after 4 weeks of high-fat feeding (**Fig. 5b**). NCR1-l upregulation was not observed in hepatocytes or adipocytes isolated from mouse subcutaneous fat (**Fig. 5b**). Immunohistological analysis of human tissues stained with NKp46-immunoglobulin fusion proteins demonstrated that VAT, but not subcutaneous fat, expressed NKp46 ligands (**Fig. 5c**).

We next investigated the effect of NCR1 stimulation on NK cell activation. *In vitro* stimulation of NK cells with agonistic NCR1 antibodies resulted in the concentration-dependent induction of IFN-γ and differentiation toward a mature CD27$^+$CD11b$^+$ NK cell phenotype (**Fig. 5d** and **Supplementary Fig. 5b**). Because the different buoyancies of NK cells and whole adipocytes make direct cocultivation of these cells complicated, we cultured NK cells with the membrane fraction of adipocytes isolated from VAT or subcutaneous fat from NCD-fed or HFD-fed mice. Adipocyte membranes from the VAT of HFD-fed mice induced a significant increase in IFN-γ production compared with membranes from the VAT of NCD-fed mice (**Fig. 5e**), whereas membranes from subcutaneous fat did not increase IFN-γ production. NK cells isolated from *Ncr1*$^{gfp/gfp}$ mice, which lack NCR1 but respond normally to other activating stimuli (ref. 21 and **Supplementary Fig. 5c**), did not show increased IFN-γ production when cultured with either type of adipocyte membrane from HFD-fed mice (**Fig. 5f**). Finally, VAT NK cells from HFD-fed mice showed increased IFN-γ production in response to NCR1 stimulation relative to VAT NK cells from NCD-fed animals (**Fig. 5g**).

We then investigated whether NCR1 stimulation of NK cells induced M1 macrophage differentiation. Macrophages cocultured with NCR1-stimulated NK cells or with supernatant from stimulated NK cells induced the expression of iNOS, as measured by flow cytometry, and this effect, as well as CD11c expression on macrophages, was blocked by the addition of neutralizing antibodies to IFN-γ (**Fig. 5h** and **Supplementary Fig. 5d**,**e**). Together, these data indicate that adipocytes from HFD-fed mice stimulate NK cells to produce IFN-γ via the induction of NCR1 ligands, and in turn IFN-γ drives M1 macrophage differentiation.

NCR1 deficiency delays development of insulin resistance

Next we investigated whether NCR1 deficiency affects HFD-induced M1 macrophage polarization *in vivo*. Changes in VAT NK cell numbers or activation were not observed in *Ncr1*$^{gfp/gfp}$ mice compared with wild-type controls at the end of 6 weeks of HFD feeding (**Fig. 6a**,**b**). HFD-fed *Ncr1*$^{gfp/gfp}$ mice had fewer M1 macrophages after 6 weeks of the HFD than did wild-type controls, a reduction similar to that seen in NK cell (antibody)-depleted mice (**Fig. 6c**). The expression of IFN-γ and TNF was greatly reduced in the VAT of HFD-fed *Ncr1*$^{gfp/gfp}$ mice and NK cell–depleted mice compared to that in wild-type HFD-fed controls (**Fig. 6d**,**e**). *Tnfrsf1a*$^{-/-}$ mice, which lack the p55 subunit of the TNF receptor, showed no reduction in the number of M1 macrophages in VAT after 6 weeks of HFD feeding (**Supplementary Fig. 6a**), which indicates that TNF produced by NK cells in response to NCR1 stimulation does not play a dominant role in this process.

We subjected *Ncr1*$^{gfp/gfp}$ and NK cell–depleted mice to prolonged HFD feeding (12 weeks) and found that NCR1 deficiency ameliorated glucose tolerance and reduced insulin resistance to a degree similar to that seen in NK cell–deficient mice (**Fig. 6f**). *Klrk1*$^{-/-}$ mice, which lack the NK cell activating receptor NKG2D, did not demonstrate reduced glucose tolerance after 12 weeks of the HFD (data not shown). NCR1-deficient and NK cell–depleted mice were obese and had increased fat pad weight compared to NCD-fed controls (**Supplementary Fig. 6b**,**c**), which indicated that NK cells

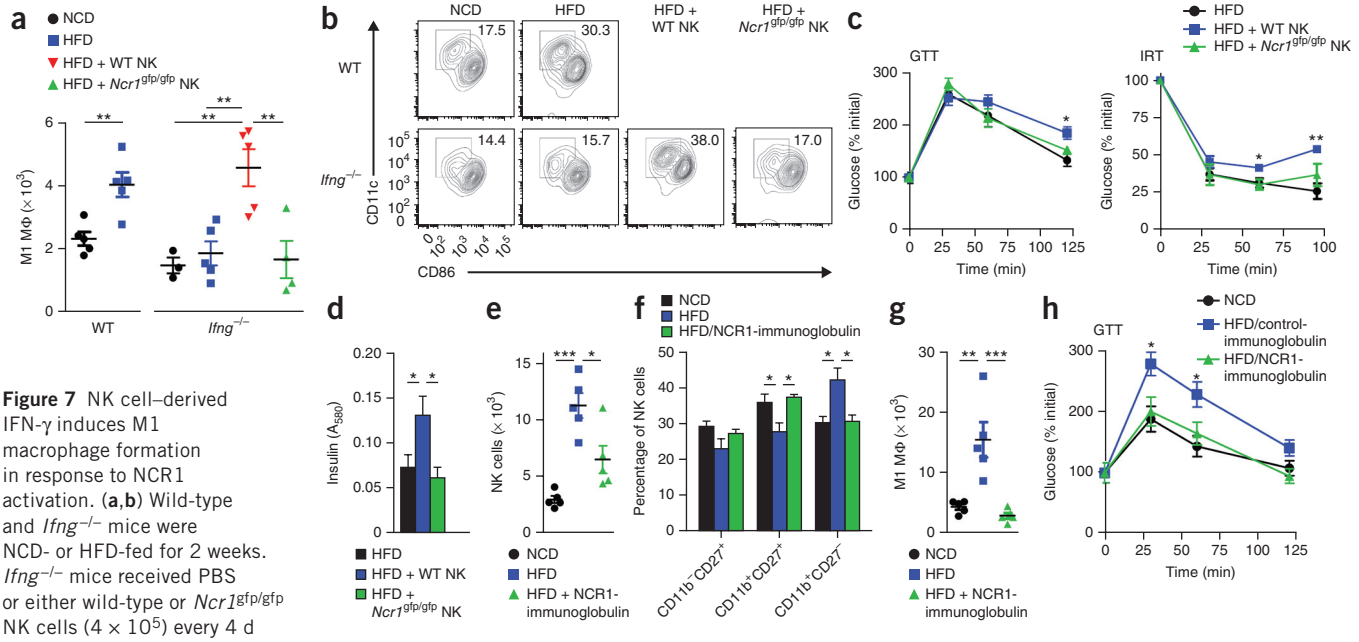

Figure 7 NK cell–derived IFN-γ induces M1 macrophage formation in response to NCR1 activation. (**a**,**b**) Wild-type and *Ifng*$^{-/-}$ mice were NCD- or HFD-fed for 2 weeks. *Ifng*$^{-/-}$ mice received PBS or either wild-type or *Ncr1*$^{gfp/gfp}$ NK cells (4×10^5) every 4 d ($n = 3$–5). (**a**) Quantification of M1 macrophages in VAT by flow cytometry. (**b**) Representative flow cytometry plots of macrophages. Gated for CD19$^-$CD11b$^+$F4/80$^+$GR1$^{Dim/-}$ cells. (**c**,**d**) *Ifng*$^{-/-}$ mice ($n = 4$–6) were HFD-fed and received PBS, WT NK cells or *Ncr1*$^{gfp/gfp}$ NK cells (4×10^5) every 4 d in the first 2 weeks and once per week for an additional 8 weeks. Next, mice were subjected to GTT and IRT (**c**). Shown are plasma glucose levels relative to the start of the HFD (time point 0, T_0). (**d**) Serum insulin levels as determined by ELISA. (**e**–**g**) Mice were NCD- or HFD-fed and injected intraperitoneally with PBS or 5 mg kg^{-1} NCR1-immunoglobulin twice per week. After 2 weeks, VAT-resident cells were analyzed by flow cytometry ($n = 5$). (**e**) Absolute number of NK cells in VAT. (**f**) VAT NK cell phenotypes. (**g**) Absolute number of M1 macrophages. (**h**) GTT results for indicated groups after 10 weeks of treatment with PBS, control-immunoglobulin or NCR1-immunoglobulin. Shown are plasma glucose levels relative to T_0 ($n = 5$). $^*P < 0.05$, $^{**}P < 0.01$, $^{***}P < 0.001$ (Student's *t*-test and ANOVA with Bonferroni's post-test). Data (±s.e.m.) are representative of one (**c**,**d**,**h**) or two (**a**,**b**,**e**–**g**) independent experiments.

mediate VAT inflammation and not VAT metabolism. To address the involvement of NCR1 in mediating systemic insulin resistance, HFD-fed wild-type, *Ncr1*$^{gfp/gfp}$ and NK cell–depleted mice were injected with PBS or insulin after being fasted overnight, and phosphorylation of signaling mediators downstream of the insulin receptor was measured in whole tissue homogenates of liver and VAT 30 min after injection. Whereas HFD-fed wild-type mice showed an impaired capacity to induce Akt phosphorylation in response to insulin in both liver and VAT, NK cells in HFD-fed *Ncr1*$^{gfp/gfp}$ mice showed p-Akt induction in amounts similar to those in NCD-fed mice (**Fig. 6g**). Similar observations were made for p-p70, p-GSK3α and p-ERK1/2 (**Supplementary Fig. 6d**). Thus, we concluded that NK cell modulation of systemic insulin resistance in response to an HFD requires NCR1.

NK cells promote M1 macrophages via IFN-γ

To further prove that NK cell–derived IFN-γ mediates the accumulation of M1 macrophages in VAT in response to NCR1 activation, we supplemented HFD-fed CD45.2$^+$ *Ifng*$^{-/-}$ mice with wild-type (CD45.1$^+$) or NCR1-deficient (GFP$^+$) NK cells by injecting the cells directly into the mouse fat pads once every 5 d during 2 weeks of HFD feeding. Transfer efficiency was confirmed by flow cytometry (**Supplementary Fig. 7a**). HFD-fed IFN-γ–deficient mice showed no accumulation of M1 macrophages in VAT without NK cell transfer (**Fig. 7a**,**b**). Transfer of CD45.1$^+$ NK cells into the fat pads of *Ifng*$^{-/-}$ mice restored M1 polarization, whereas transfer of NCR1-deficient NK cells did not (**Fig. 7a**). As reported previously[26–28], prolonged HFD feeding in IFN-γ–deficient mice resulted in reduced glucose intolerance relative to that of wild-type mice (**Supplementary Fig. 7b**). Transfer of CD45.1$^+$, but not of NCR1-deficient, NK cells once every week via injection into the fat pad significantly impaired glucose tolerance and increased insulin resistance and plasma insulin amounts during prolonged (10 weeks) feeding with an HFD (**Fig. 7c**,**d**). When CD45.1$^+$ NK cells were injected intravenously into HFD-fed IFN-γ–deficient mice, very few donor NK cells reached the VAT, and the donor NK cells that could be detected in this tissue did not acquire the CD69$^+$CD62L^{dim} phenotype of resident NK cells at 2 weeks after transfer (**Supplementary Fig. 7c**). Intravenously injected donor CD45.1$^+$ NK cells were not found to drive M1 macrophage polarization in the VAT of IFN-γ–deficient mice at 2 weeks after transfer (**Supplementary Fig. 7d**). Thus, we concluded that IFN-γ from tissue-resident NK cells is required for M1 macrophage polarization in the VAT and the induction of glucose intolerance during HFD feeding.

Finally, we investigated whether proinflammatory M1 macrophage accumulation and glucose intolerance could be prevented by a therapeutic protocol that prevents NCR1 activation. Because many blocking antibodies to NCR1 can also stimulate this protein, depending on the way in which they are presented, NCR1 antibodies cannot be used *in vivo* (**Supplementary Fig. 7e**). Therefore, mice on an HFD were injected twice per week with NCR1-immunoglobulin fusion proteins that specifically blocked NCR1 ligands (ref. 22 and **Supplementary Fig. 7f**–**h**). NCR1-l blocking prevented the activation and accumulation of NK cells in VAT after 2 weeks of HFD feeding, prevented M1 macrophage accumulation to a degree similar to that observed in NCR1-deficient mice, and reversed the ratio of M1 to M2 macrophages (**Fig. 7e**–**g** and **Supplementary Fig. 7i**–**k**). Moreover, NCR1-immunoglobulin administration during prolonged (10 weeks) HFD feeding was able to prevent glucose intolerance in response to prolonged high-fat feeding, whereas diet-induced weight gain remained unaltered (**Fig. 7h** and **Supplementary Fig. 7l**). In conclusion,

NK cell–derived IFN-γ was found to drive early obesity-induced M1 macrophage polarization in response to NCR1 activation.

DISCUSSION

Current clinical practice aims for earlier and more preventive treatment of patients with type 2 diabetes[39]. The inflammatory environment in obese VAT is an important underlying cause of insulin resistance and is responsible for many of the most life-threatening pathologies associated with type 2 diabetes[40]. In recent years, numerous obesity-induced adipose stress factors[11,12,41,42] and immune cells that perpetuate VAT inflammation[4,14,16,31] have been characterized. The accumulation of proinflammatory M1 macrophages in obese VAT is a key event in disease development, and its prevention is therefore an attractive target for early treatment. Here we have identified one of the primary immunological links between adipose tissue stress and M1 macrophage accumulation. Diet-induced obesity induces the upregulation of NCR1 ligand expression in adipose tissue, which activates VAT-resident NK cells to produce IFN-γ and thereby drive M2-to-M1 macrophage polarization. This results in VAT inflammation and ultimately leads to insulin resistance.

Under lean conditions, anti-inflammatory immune cells such as *i*NKT cells, ILC2 cells and eosinophils predominate in VAT and maintain homeostasis through the production of T_H2-type cytokines[6–9]. Within the first few days of high-fat feeding, the increase in metabolites (for example, free fatty acids, palmitate and ceramides) and an influx of neutrophils in VAT mediate an increase in the number of macrophages in this tissue, mostly through local proliferation[11,15,37,43]. Prolonged HFD feeding causes VAT macrophages to acquire a proinflammatory phenotype that is enhanced by the increased accumulation of B cells and $CD8^+$ T cells in the tissue[14,16]. Although we observed an increase in the number of NK cells within days after the start of HFD feeding (data not shown), NK cells reached their maximum accumulation only after 2 weeks. We speculate that the expression of NCR1 ligands in VAT needs to exceed a certain threshold in order to overcome NK cell control by inhibitory stimuli. When NK cells were depleted, or in NCR1-deficient mice, macrophage numbers still increased in the VAT after HFD feeding, but they lacked the IFN-γ–mediated signal to differentiate into M1 macrophages. Thus, whereas various stress factors contribute to inflammation and increased numbers of macrophages in obese VAT within the first few days of an HFD, NK cells are needed to provide the immunological licensing that allows macrophages to achieve their full proinflammatory potential[44]. This system might ensure that HFDs are able to lead to pathology only after a feed-forward signal is received from NK cells.

NK cells are also subject to immunological control, especially by activated macrophages[45]. Moreover, resting human NK cells require additional stimuli to be activated by NCR1 engagement[46]. We did not find induction of NKG2D ligands on obese adipocytes. Nevertheless, it could be interesting to investigate whether additional NK cell–activating molecules are differentially expressed on metabolically stressed adipocytes. In contrast, lean-tissue VAT NK cells have high expression of CD69 and readily produced IFN-γ after NCR1 stimulation *in vitro*. This corresponds with an activated phenotype and implies that the cells require few additional stimuli in order to be sensitized by stressed adipocytes. Nevertheless, we consider it likely that, in addition to NCR1 activation, NK cell activation can be promoted by multiple activating stimuli acquired through reciprocal communication with various cells that are activated early in diet-induced obesity.

The interaction between NK cells and adipose tissue is in accordance with recent insights that recognize the key role of adipocytes in metabolic disease. Whereas adipocytes were long regarded as static nutrient-storage depots, they are currently appreciated as important endocrine cells[10]. Adipocytes excrete a multitude of soluble factors, generally referred to as adipokines, which regulate the metabolic responses of many organs, including the liver, brain and pancreas[47]. In addition, adipokines can stimulate or dampen inflammation locally. An HFD results in acute hypertrophy of adipocytes[48], which causes cellular stress of adipocytes and their stroma due to microhypoxia[12], endoplasmic reticulum stress and extracellular matrix confinement[13]. This drives an increase in the amount of proinflammatory adipokines in VAT, which leads to the accumulation and activation of immune cells. NK cells are important innate sensors of cellular stress caused by viral infection and oncogenic transformation[19]. Their activity is controlled by a careful balance of extracellular cues that they receive via a range of activating and inhibitory receptors. Direct cell-cell contact between immune cells and adipocytes has so far been poorly studied. Here we show that adipocytes directly communicate their stress to resident NK cells by upregulating the expression of NCR1 ligands. This signal is sufficient to activate NK cells and promote their proliferation and production of macrophage-polarizing cytokines. Our findings are in line with published findings demonstrating that VAT in obese people contains considerably more NK cells and has higher expression of IFN-γ than does subcutanous fat[26,49].

In conclusion, our study identified an important new immunological link between obesity and proinflammatory macrophage differentiation in obese VAT involving the activation of NK cells by stressed adipocytes. The NK cell–macrophage axis in adipose tissue therefore is a promising new target for the treatment of patients with metabolic syndrome to reduce the risk of progression to type 2 diabetes.

METHODS

Methods and any associated references are available in the online version of the paper.

Note: Any Supplementary Information and Source Data files are available in the online version of the paper.

ACKNOWLEDGMENTS

We thank S. Slavić-Stupac, M. Samsa and K. Miklić for technical assistance and D. Jurišić-Eržen and M. Zelić for help with study setup. Supported by the European Foundation for the Study of Diabetes (New Horizons Program), the Unity through Knowledge Fund (15/13 to B.P.), the University of Rijeka (13.06.1.1.03 to B.P.), the Netherlands Organization for Scientific Research (91614029 to F.M.W.) and the European Commission (PCIG14-GA-2013-630827 to F.M.W.).

AUTHOR CONTRIBUTIONS

F.M.W. designed and carried out most of the experiments and analyzed data. V.J., S.V., M.Š., T.T.W. and V.S. performed and analyzed experiments. A.G. generated key research reagents. D.M. obtained informed consent from patients and obtained human samples. D.Š. supervised the setup of the clinical study. F.T.W. and J.C.B. coordinated the metabolic studies. O.M. helped design studies with NCR^{GFP} mice. B.P. directed the research and wrote the paper with F.M.W., with input from all coauthors.

COMPETING FINANCIAL INTERESTS

The authors declare no competing financial interests.

1. Stevens, G.A. *et al.* National, regional, and global trends in adult overweight and obesity prevalences. *Popul. Health Metr.* **10**, 22 (2012).
2. Danaei, G. *et al.* National, regional, and global trends in fasting plasma glucose and diabetes prevalence since 1980: systematic analysis of health examination surveys and epidemiological studies with 370 country-years and 2.7 million participants. *Lancet* **378**, 31–40 (2011).
3. Xu, H. *et al.* Chronic inflammation in fat plays a crucial role in the development of obesity-related insulin resistance. *J. Clin. Invest.* **112**, 1821–1830 (2003).

4. Weisberg, S.P. *et al.* Obesity is associated with macrophage accumulation in adipose tissue. *J. Clin. Invest.* **112**, 1796–1808 (2003).
5. Hotamisligil, G.S. Inflammation and metabolic disorders. *Nature* **444**, 860–867 (2006).
6. Lynch, L. *et al.* Adipose tissue invariant NKT cells protect against diet-induced obesity and metabolic disorder through regulatory cytokine production. *Immunity* **37**, 574–587 (2012).
7. Molofsky, A.B. *et al.* Innate lymphoid type 2 cells sustain visceral adipose tissue eosinophils and alternatively activated macrophages. *J. Exp. Med.* **210**, 535–549 (2013).
8. Schipper, H.S. *et al.* Natural killer T cells in adipose tissue prevent insulin resistance. *J. Clin. Invest.* **122**, 3343–3354 (2012).
9. Wu, D. *et al.* Eosinophils sustain adipose alternatively activated macrophages associated with glucose homeostasis. *Science* **332**, 243–247 (2011).
10. Cao, H. Adipocytokines in obesity and metabolic disease. *J. Endocrinol.* **220**, T47–T59 (2014).
11. Shi, H. *et al.* TLR4 links innate immunity and fatty acid-induced insulin resistance. *J. Clin. Invest.* **116**, 3015–3025 (2006).
12. Ye, J., Gao, Z., Yin, J. & He, Q. Hypoxia is a potential risk factor for chronic inflammation and adiponectin reduction in adipose tissue of ob/ob and dietary obese mice. *Am. J. Physiol. Endocrinol. Metab.* **293**, E1118–E1128 (2007).
13. Khan, T. *et al.* Metabolic dysregulation and adipose tissue fibrosis: role of collagen VI. *Mol. Cell. Biol.* **29**, 1575–1591 (2009).
14. Winer, D.A. *et al.* B cells promote insulin resistance through modulation of T cells and production of pathogenic IgG antibodies. *Nat. Med.* **17**, 610–617 (2011).
15. Talukdar, S. *et al.* Neutrophils mediate insulin resistance in mice fed a high-fat diet through secreted elastase. *Nat. Med.* **18**, 1407–1412 (2012).
16. Nishimura, S. *et al.* CD8$^+$ effector T cells contribute to macrophage recruitment and adipose tissue inflammation in obesity. *Nat. Med.* **15**, 914–920 (2009).
17. Borst, S.E. The role of TNF-alpha in insulin resistance. *Endocrine* **23**, 177–182 (2004).
18. Patsouris, D. *et al.* Ablation of CD11c-positive cells normalizes insulin sensitivity in obese insulin resistant animals. *Cell Metab.* **8**, 301–309 (2008).
19. Vivier, E. *et al.* Innate or adaptive immunity? The example of natural killer cells. *Science* **331**, 44–49 (2011).
20. Shi, F.D., Ljunggren, H.G., La Cava, A. & Van Kaer, L. Organ-specific features of natural killer cells. *Nat. Rev. Immunol.* **11**, 658–671 (2011).
21. Gazit, R. *et al.* Lethal influenza infection in the absence of the natural killer cell receptor gene *Ncr1*. *Nat. Immunol.* **7**, 517–523 (2006).
22. Gur, C. *et al.* The activating receptor NKp46 is essential for the development of type 1 diabetes. *Nat. Immunol.* **11**, 121–128 (2010).
23. Mosser, D.M. & Edwards, J.P. Exploring the full spectrum of macrophage activation. *Nat. Rev. Immunol.* **8**, 958–969 (2008).
24. Goldszmid, R.S. *et al.* NK cell-derived interferon-gamma orchestrates cellular dynamics and the differentiation of monocytes into dendritic cells at the site of infection. *Immunity* **36**, 1047–1059 (2012).
25. Han, M.S. *et al.* JNK expression by macrophages promotes obesity-induced insulin resistance and inflammation. *Science* **339**, 218–222 (2013).
26. O'Rourke, R.W. *et al.* Systemic inflammation and insulin sensitivity in obese IFN-gamma knockout mice. *Metabolism* **61**, 1152–1161 (2012).
27. Wong, N. *et al.* Deficiency in interferon-gamma results in reduced body weight and better glucose tolerance in mice. *Endocrinology* **152**, 3690–3699 (2011).
28. Rocha, V.Z. *et al.* Interferon-gamma, a Th1 cytokine, regulates fat inflammation: a role for adaptive immunity in obesity. *Circ. Res.* **103**, 467–476 (2008).
29. Hayakawa, Y. & Smyth, M.J. CD27 dissects mature NK cells into two subsets with distinct responsiveness and migratory capacity. *J. Immunol.* **176**, 1517–1524 (2006).
30. Klose, C.S. *et al.* Differentiation of type 1 ILCs from a common progenitor to all helper-like innate lymphoid cell lineages. *Cell* **157**, 340–356 (2014).
31. Feuerer, M. *et al.* Lean, but not obese, fat is enriched for a unique population of regulatory T cells that affect metabolic parameters. *Nat. Med.* **15**, 930–939 (2009).
32. Waggoner, S.N., Cornberg, M., Selin, L.K. & Welsh, R.M. Natural killer cells act as rheostats modulating antiviral T cells. *Nature* **481**, 394–398 (2012).
33. Feng, B. *et al.* Clodronate liposomes improve metabolic profile and reduce visceral adipose macrophage content in diet-induced obese mice. *PLoS ONE* **6**, e24358 (2011).
34. Blunt, T. *et al.* Defective DNA-dependent protein kinase activity is linked to V(D)J recombination and DNA repair defects associated with the murine scid mutation. *Cell* **80**, 813–823 (1995).
35. Wong, R.H. *et al.* A role of DNA-PK for the metabolic gene regulation in response to insulin. *Cell* **136**, 1056–1072 (2009).
36. Ballak, D.B. *et al.* Combined B- and T-cell deficiency does not protect against obesity-induced glucose intolerance and inflammation. *Cytokine* **62**, 96–103 (2013).
37. Amano, S.U. *et al.* Local proliferation of macrophages contributes to obesity-associated adipose tissue inflammation. *Cell Metab.* **19**, 162–171 (2014).
38. Zafirova, B., Wensveen, F.M., Gulin, M. & Polic, B. Regulation of immune cell function and differentiation by the NKG2D receptor. *Cell. Mol. Life Sci.* **68**, 3519–3529 (2011).
39. Inzucchi, S.E. *et al.* Management of hyperglycaemia in type 2 diabetes: a patient-centered approach. Position statement of the American Diabetes Association (ADA) and the European Association for the Study of Diabetes (EASD). *Diabetologia* **55**, 1577–1596 (2012).
40. Johnson, A.R., Milner, J.J. & Makowski, L. The inflammation highway: metabolism accelerates inflammatory traffic in obesity. *Immunol. Rev.* **249**, 218–238 (2012).
41. Ozcan, U. *et al.* Endoplasmic reticulum stress links obesity, insulin action, and type 2 diabetes. *Science* **306**, 457–461 (2004).
42. Houstis, N., Rosen, E.D. & Lander, E.S. Reactive oxygen species have a causal role in multiple forms of insulin resistance. *Nature* **440**, 944–948 (2006).
43. Haus, J.M. *et al.* Plasma ceramides are elevated in obese subjects with type 2 diabetes and correlate with the severity of insulin resistance. *Diabetes* **58**, 337–343 (2009).
44. Aouadi, M. *et al.* Gene silencing in adipose tissue macrophages regulates whole-body metabolism in obese mice. *Proc. Natl. Acad. Sci. USA* **110**, 8278–8283 (2013).
45. Tripp, C.S., Wolf, S.F. & Unanue, E.R. Interleukin 12 and tumor necrosis factor alpha are costimulators of interferon gamma production by natural killer cells in severe combined immunodeficiency mice with listeriosis, and interleukin 10 is a physiologic antagonist. *Proc. Natl. Acad. Sci. USA* **90**, 3725–3729 (1993).
46. Bryceson, Y.T., March, M.E., Ljunggren, H.G. & Long, E.O. Synergy among receptors on resting NK cells for the activation of natural cytotoxicity and cytokine secretion. *Blood* **107**, 159–166 (2006).
47. Ouchi, N., Parker, J.L., Lugus, J.J. & Walsh, K. Adipokines in inflammation and metabolic disease. *Nat. Rev. Immunol.* **11**, 85–97 (2011).
48. Wang, Q.A., Tao, C., Gupta, R.K. & Scherer, P.E. Tracking adipogenesis during white adipose tissue development, expansion and regeneration. *Nat. Med.* **19**, 1338–1344 (2013).
49. Huebner, L. *et al.* Human NK cell subset functions are differentially affected by adipokines. *PLoS ONE* **8**, e75703 (2013).

ONLINE METHODS

Mice. Mice were strictly age- and sex-matched within experiments and were handled in accordance with institutional, national and/or EU guidelines. Wild-type C57BL/6 (strain 000664), *Prkdc*^{scid} (strain 001913), *Ifng*$^{-/-}$ (strain 002287) and *Tnfrsf1a*$^{-/-}$ (strain 003242) mice were from the Jackson Laboratory. *Ncr1*$^{gfp/gfp}$ mice have been described[21] and were provided by O.M. (Hebrew University Hadassah Medical School). Heterozygous *Ncr1*$^{gfp/+}$ mice were used in transfer experiments using GFP-labeled NK cells. All genetically modified animal models were generated in C57BL/6 mice or backcrossed at least ten times on this background. Male mice (8–12 weeks old) were fed *ad libitum* with an NCD (Mucedola) or an HFD in which 50% of calories were derived from animal fat (Bregi). All lines were kept as breeding colonies in the local animal facility in Rijeka, Croatia, under specific pathogen-free conditions. All animal experiments were done with approval from the University of Rijeka Medical Faculty Ethics Committee.

Glucose tolerance and insulin resistance tests. For glucose tolerance tests (GTTs), mice were fasted for 6–12 h. Next, mice were injected i.p. with 1.0 g/kg glucose. Before and up to 120 min after injection, blood glucose concentrations were measured in venous blood (Vena Saphena) using an automated glucometer (LifeScan). For insulin resistance tests (IRTs), blood glucose values were determined and animals were injected with 1.0 U/kg fast-working human insulin (Eli Lilly). Venous blood glucose concentrations were determined up to 90 min after injection.

Isolation of leukocytes from VAT and *in vitro* killer assay. White adipose tissue was excised and cut in small pieces with a scalpel. Cut tissues were put in DMEM containing 1 mg/ml Collagenase D (Sigma-Aldrich) and incubated for 1 h at 37 °C with shaking. Suspensions were thoroughly vortexed and subsequently centrifuged (500*g* for 5 min). The pellet was resuspended in a hypotonic solution (155 mM NH_4Cl, 10 mM $KHCO_3$, 1 mM EDTA) and run through a sieve to remove remaining cell debris. Cells were centrifuged and resuspended in PBS containing 1% BSA. For the *in vitro* killer assay, the fraction of NK cells in total splenocytes or VAT leukocytes was determined by flow cytometry. Cells were mixed with CFSE-labeled target cells (YAC-1), in the indicated ratios (**Supplementary Fig. 1e**), in the presence of 1,000 U/ml IL-2 (R&D Systems). After 5 h, the fraction of killed target cells was determined by To-Pro3 staining and flow cytometric analysis.

Antibodies. For flow cytometry, we used monoclonal antibodies to mouse CD4 (L3T4), CD3 (17A2), CD8-β (eBioH35-17.2), CD19 (eBio1D3), CD25 (PC61.5), CD44 (IM7), CD45.1 (A20), CD62L (MEL-14), CD94 (18D3), CD122 (5H4), CD127 (A7R34), KLRG1 (2F1), Ly49a (A1), Ly49g2 (AT8), NK1.1 (PK136), T-Bet (eBio4B10), CD117 (ACK2), TRAIL (N2B2), Eomes (Dan11mag), CD49b (DX5), CD27 (LG.7F9), CD11b (M1/70), CD11c (N418), CD86 (GL1), NKG2D (CX5), NCR1 (29A1.4), NKG2A/C/E (20D5), GR1 (RB6-8C5), Ly49h (3D10), Ly49i (YLI-90), Ly49c/i (5E6), CD103 (2E7), CD93 (AA4.1), CD48 (HM48-1), CXCR3 (CXCR3-173), F4/80 (BM8), γδ TCR (eBioGL3), FoxP3 (FJK-16S), NOS2 (CXNFT) and CD69 (H1.2F3) from eBioscience. Antibodies to 2B4 (2B4), CD51 (RMV-7), CD107a (1D4B), Ly49D (4E5), CD124 (mIL4R-M1), BrdU (B44) and IFN-γ (XMG1.2) were from BD Biosciences. Antibody to arginase was from R&D Research (IC5868F). Antibodies for *in vivo* applications (CD4 (YTS191.1.2), CD8 (YTS169.4.2), NK1.1 (PK136), IFN-γ (R4-6A2) and isotype controls) were produced by our in-house facility at the University of Rijeka and chromatography-purified or purchased from BioXcell. The neutralization capacity of IFN-γ antibodies was determined as described[50].

Flow cytometry. Cells were pretreated with Fc block (clone 2.4G2, produced in-house at the University of Rijeka) and analyzed in the presence of propidium iodide (Sigma-Aldrich) or To-Pro3 (Life Technologies) to distinguish live cells. Cells were stained and analyzed in PBS containing 1% BSA and NaN_3. Staining of nuclear proteins was done with the FoxP3 staining buffer set (eBioscience). For IFN-γ staining, cells were first stimulated for 5 h *in vitro* with 1,000 U/ml IL-2 (R&D Systems) in the presence of PMA and ionomycin (Sigma-Aldrich) or plate-bound NCR1 or NK1.1 antibodies and Brefeldin A (eBioscience). For non-nuclear intracellular staining, permeabilization and fixation of cells was done with the Fix/Perm kit (BD Biosciences). Most flow cytometry experiments were done on a FACSverse or FACSaria (BD Biosciences). Adipocytes were measured using a low-pressure system on a FACScalibur (BD Biosciences). FCS files were analyzed with FlowJo software (TriStar).

Immunohistology. Tissues were fixed in 4% formalin for 24 h, dehydrated and embedded in paraffin. Sections (2 µm) were deparaffinized and stained using hNKp46-immunoglobulin, mNCR1-immunoglobulin or mNKG2D-immunoglobulin fusion proteins as described[22]. Boiling in citrate buffer was used as an antigen-retrieval method. Irrelevant immunoglobulin fusion proteins were used as negative controls. Fusion proteins were detected by incubation with antibody to human IgG conjugated to peroxidase (Sigma-Aldrich). Staining was visualized with DAB (Dako) and brief hematoxylin counterstaining. Staining was quantified using ImageJ software (NIH).

Immunoblot and ELISA. Mice were fasted overnight and subsequently injected i.p. with 1 U/kg human insulin (Novartis). After 30 min, liver and VAT were isolated and snap-frozen in liquid nitrogen. Tissue extracts were generated using a Triton lysis buffer (50 mM HEPES, 1% Triton X-100, 100 mM NaF, 10 mM Na-orthovanadate, 10 mM EDTA, 0.1% SDS, 50 mM NaCl, 0.67% aprotinin, 0.2% benzamidin, pH 7.4) in a tissue homogenizer. Extracts (30 µg) were analyzed with polyclonal antibodies to pAkt (Ser^{473}), p-p70 (Thr^{389}), pERK1/2 (Thr^{202}/Tyr^{204}), pGSK3-α ($Ser^{21/9}$), Pan-ERK1/2, calnexin and β-actin from Cell Signaling. Quantification of signal was done with ImageJ software (NIH). Serum insulin levels were quantified by sandwich ELISA with capture (D6C4, Acris Antibodies) and biotinylated detection antibody (D3E7, Acris Antibodies).

***In vivo* experiments.** For VATectomy, mice were anesthetized with isoflurane, and abdominal hair was removed with depilation cream (Veet). The abdomen was opened with a small Pfannenstiel incision. For sham operations, abdominal fat pads were taken out of the abdomen and then replaced. For VATectomy, abdominal fat pads were surgically removed. Animals were closed, and stitches were removed 1 week after surgery. Two weeks after surgery, animals were put on either a normal or a high-fat diet. For adoptive transfers, mice were pretreated with $CD4^+$- and $CD8^+$-cell–depleting antibodies. After 24 h, spleens were isolated. NK cells were purified with biotinylated DX5 antibodies, streptavidin-coated beads and magnetic cell sorting (Miltenyi). Purity was confirmed by flow cytometry. In the IFN-γ–sufficient NK cell–supplementation experiment, 4×10^5 NK cells were transferred once every 4 d in the first 2 weeks and once every week in the 10 weeks thereafter. For long-term BrdU incorporation, mice were NCD- or HFD-fed for 2 weeks and injected i.p. with 0.8 mg BrdU every other day for 8 d before analysis. For short-term BrdU incorporation, mice were injected i.p. with 2 mg BrdU and killed after 4 h. BrdU incorporation was analyzed using the BrdU Flow Kit (BD Biosciences). For blocking of NCR1 ligands, mice were injected twice per week with NCR1-immunoglobulin or irrelevant fusion proteins (0.005 g/kg) as described[22]. For macrophage depletion, mice were injected once every 2 weeks with 45 mg/kg clodronate-loaded or unloaded control liposomes (ClodronateLiposomes.com).

Cocultivation assays. For NK cell–adipocyte membrane cocultures, adipose tissue was excised and directly incubated for 1 h at 37 °C in DMEM containing 1 mg/ml Collagenase D (Sigma-Aldrich) with shaking. Suspensions were centrifuged at low speed (5 min, 200*g*), and adipocytes were isolated from the top fraction. Cells were washed twice with ice-cold PBS and resuspended in a small volume. Cells were fractionated by three cycles of snap-freezing and rapid thawing followed by vortexing. The adipocyte membrane fraction was obtained by subsequent centrifuging (5 min, 12,000*g*). Membrane content was normalized based on optical density. NK cells were cocultured with membranes for 5 h in the presence of Brefeldin A. For macrophage polarization assays, peritoneal macrophages were mixed in a 1:1 ratio with NK cells activated with plate-bound NCR1 antibodies. Alternatively, macrophages were cultured with supernatants of NK cells activated for 48 h with NCR1 antibodies. IFN-γ was neutralized with antibodies in the presence of Fc block. Macrophages were cultured for 2 d, the last 5 h of which were in the presence of Brefeldin A, and then subjected to intracellular iNOS staining. For analysis of macrophage polarization, the total stromal-vascular fraction of VAT was stimulated for 2 d with NCR1 antibodies.

RNA. White adipose tissue was excised and cut in small pieces with a scalpel. Cut tissues were suspended in DMEM containing 1 mg/ml Collagenase D (Sigma-Aldrich) and incubated for 1 h at 37 °C with shaking. Suspensions were thoroughly vortexed, and a small fraction was directly dissolved in Trizol. RNA was isolated via the Trizol method, and cDNA was generated with a reverse transcriptase core kit (Eurogentec). The expression of mRNA was examined by quantitative PCR analysis with a 7500 Fast Real Time PCR machine. Taqman assays were used to quantify the expression of *Emr1* (F4/80, Mm00802529_m1), *Itgax* (CD11c, Mm00498698_m1), *Tnf* (TNF, Mm00443260_g1), *Il1b* (IL-1β, Mm00434228_m1) and *Ifng* (IFN-γ, Mm00485148_m1). The relative mRNA expression was normalized by quantification of *Rn18S* (18S, Mm03928990_g1) RNA in each sample.

Human samples. Human tissues were obtained from patients undergoing elective laparoscopic cholecystectomy. Patients who had inflamed gall bladders during surgery were excluded from the study. All patients signed an informed consent form before tissues were isolated, and the study received approval from the University of Rijeka Medical Faculty Ethics Committee before it was started.

Statistics. Figures represent means and s.e.m. (depicted by error bars). To analyze statistical significance, we used Student's *t*-test, Mann-Whitney, Kruskal-Wallis and ANOVA, with Bonferroni's post-test correction for multiple comparisons. $P < 0.05$ was considered statistically significant.

50. Polić, B. *et al*. Hierarchical and redundant lymphocyte subset control precludes cytomegalovirus replication during latent infection. *J. Exp. Med.* **188**, 1047–1054 (1998).

doi:10.1038/ni.3120